Journal of ELECTRONIC MATERIALS, Vol. 36, No. 9, 2007 Regular Issue Paper
DOI: 10.1007/s11664-007-0122-8
© 2007 TMS

Damage Produced in Solder Alloys during Thermal Cycling

X.W. LIU[1,3] and W.J. PLUMBRIDGE[2]

1.—Science and Technology Research Institute (STRI), University of Hertfordshire, Hatfield, Herts, AL10 9AB, UK. 2.—Solder Research Group, Department of Materials Engineering, The Open University, Milton Keynes, MK7 6AA, UK. 3.—e-mail: W.Plumbridge@open.ac.uk

The anisotropy of tin is associated with significant variations in its coefficient of thermal expansion and elastic modulus, with crystallographic direction. Under pure thermal cycling (with no externally applied stress or strain), substantial strains, in excess of 100%, may develop locally, and for very small structures, such as soldered interconnections comprising a few grains, structural integrity may be adversely affected. To examine this possibility, *freestanding* samples of tin, Sn-3.5wt.%Ag, Sn-0.5wt.%Cu, and Sn-3.8wt.%Ag-0.7wt.%Cu, have been subjected to thermal cycling. Temperature cycles from 30°C to 125°C or from −40°C to 55°C initially caused surface cracking, with openings up to several tens of microns after 3,000 cycles. Subsequently, the surface cracks grew into the interior of the specimens, with the maximum penetration ranging from a few microns after 100 cycles to more than 200 μm after 3,000 cycles. The cracks initiated from damage accumulated along grain boundaries. For the same temperature range, less damage resulted after the lower maximum (or mean) temperature cycle, and there appears to be a thermally activated component of cracking. The microstructure produced by rapid cooling (water quenching) was slightly more resistant than that formed by air, or furnace, cooling. Apart from microstructural coarsening, no damage accrues from isothermal exposure alone.

Key words: Lead-free solders, anisotropy of tin, thermal cycling, cracks, fatigue

INTRODUCTION

Throughout their service lives, solder joints in electronic packages experience thermomechanical fatigue (TMF), which arises from the thermal expansion mismatch between the component and substrate,[1] and this constitutes a major cause of failure, especially in surface mount configurations. When the temperature of the package changes, due to either the external environment or to internal power variations, the mismatch is accommodated mainly by plastic displacement in the solder, and this repeated displacement leads to fatigue failure in shear, involving crack initiation and growth.[2] Thermomechanical fatigue in solder joints has been usually regarded as a thermally induced mechanical problem and investigated either by isothermal mechanical cycling or by cycling with both thermal and mechanical loading.[3–14] Under such conditions, the combined thermal and mechanical effects are influential. However, purely thermal effects, in the absence of any externally applied stress or strain, have been less studied.

The TMF life of the traditional solder alloy, Sn-37wt.%Pb, has been investigated using model solder joints whose regular geometry permits accurate determination of stress and strain.[2] The endurance was found to be inferior to that obtained in isothermal mechanical cycling, with the same strain ranges and temperature extremes of the thermal cycle. It was suggested that cycling the temperature alone produced degradation of both solder and solder joint and that a significant component of damage arose solely from temperature fluctuations. The situation has been investigated and analyzed on a single and three-dimensional basis, in terms of various combinations of orientation in

(Received September 13, 2006; accepted February 12, 2007; published online July 4, 2007)

Table I. Anisotropy of Tin in Thermal Expansion and Young's Modulus [15]

Direction	α, $\times 10^{-6}$/K	*E*, GPa
<100>	15.4	54.1
<101>	18.9	48.1
<111>	20.5	25.5
<113>	24.2	42.3
<001>	30.5	84.7
<110>	15.4	26.3

adjacent grains.[15,16,17] It was shown that substantial stresses can build up at grain boundaries, leading to grain boundary sliding or decohesion. Loss of joint strength during thermal cycling was attributed to the development and growth of microcracks; deformation effects, such as cyclic softening, were not considered. Three potential components of damage to soldered joints under thermal cycling have been identified as *intrinsic* (inherent in the solder itself), *contact* (arising when dissimilar materials are joined together), and *geometrical* (arising from the arrangement of neighboring joints on a board).[18]

Tin exists as β-tin having a body-centered-tetragonal structure with a = 0.58318 nm, c = 0.31818 nm, and a c/a ratio of 0.5456.[19] This structure exhibits significant anisotropy in its thermal and elastic properties, as listed in Table I. The maximum difference in thermal expansion exists between the crystalline orientations <100> and <001>, which results in a thermal expansion mismatch of 15.1×10^{-6}/K. For polycrystalline tin, with a temperature variation of 95°C, for two grains having a <100>/<001> contact, the thermal expansion mismatch will produce a strain of 0.14% along the grain boundary. The anisotropy in elasticity can result in a difference in Young's modulus of 30.6 GPa between <100> and <001>. This produces nonuniformity in the displacement of grains when they are in contact, and stresses are built up along grain boundaries when the grains are strained. The shear strain, γ, increases with the inverse of the distance to grain boundary, h ($\gamma = D/h$), where D is the displacement along grain boundary, ranging from about 1% at h = 1 μm to several tens of percent at h = 0.1 μm under the current cycling conditions. According to the orientation combination, the shear strain may vary by a factor of about 5.

In the above context, this paper considers intrinsic damage and reports the responses of pure tin, Sn-3.8wt.%Ag, Sn-0.7wt.%Cu, and Sn-3.5wt.%Ag-0.5wt.%Cu to thermal cycling. In the transition to lead-free soldering technology, these alloys are among the favorites to replace Sn-37wt.%Pb. Emphasis is placed upon the nature and extent of the damage produced and the role of parameters, such as microstructure (prior history) and service conditions, which might affect performance. It is believed that intrinsic behavior is likely to become more significant as miniaturization of electronics continues and solder joints comprise fewer grains.

EXPERIMENTAL DETAILS

The specimens used were solder blocks with the dimensions of 2 mm × 10 mm × 12 mm, replicating the solder geometry in a model joint, used in previous studies.[2] To make a sample, commercial grade solder was heated at 280°C for 10 min followed by casting in a die. Samples were water quenched from 280°C to 20°C, and the cooling rate was 80°C s^{-1}, as determined by a thermocouple embedded in the solder. They were then stored in a freezer at −20°C and removed for room-temperature storage 15 h before testing. One of the external faces of the solder blocks was polished before testing.

Thermal cycling involved a 1 h ramp up from room temperature to 125°C and a 1 h cooling to 30°C, with no dwell at the extremes. Subsequent cycles were between these temperature limits. After thermal cycling, the samples were examined by scanning electron microscope. The cracks observed on the surface are described in terms of crack *length*. To reveal the extent of cracking into the material, some samples were sectioned and polished after thermal cycling, and the cracks observed on the sectioned surface are described in terms of crack *depth*. Preliminary tests demonstrated that metallographic preparation did not cause any surface damage and affect the observations.

RESULTS AND DISCUSSION

The findings reported here relate mainly to the ternary Sn-Ag-Cu alloy, which is likely to become the most popular lead-free alloy. Observations on the other alloys and pure tin are made largely for comparative purposes.

Damage Produced during Thermal Cycling from 30°C to 125°C

Subjecting free-standing samples of pure tin, and common lead-free solders, to thermal cycling results in fatigue failure, via crack initiation and growth. Figure 1 is an overall view of the development of cracks in a Sn-3.8wt.%Ag-0.7wt.%Cu block sample during thermal cycling. Figure 1a shows the solder before test. After 100 cycles, cracks have been formed, which spread over the surface (Fig. 1b). The total surface length of all cracks is 4,640 μm. On further cycling from 100 to 1,000 cycles (Fig. 1c), and then to 3,000 cycles (Fig. 1d), the opening of the existing cracks increased and surface fragmentation of the solder occurred, suggesting crack growth into the interior of the specimen. After 3,000 cycles, the total length of cracks was 5,950 μm, not significantly greater (28%) than that after 100 cycles. Cracks that had initiated in the early stage of thermal cycling had opened and penetrated into the sample, rather than extended along the surface subsequently. The

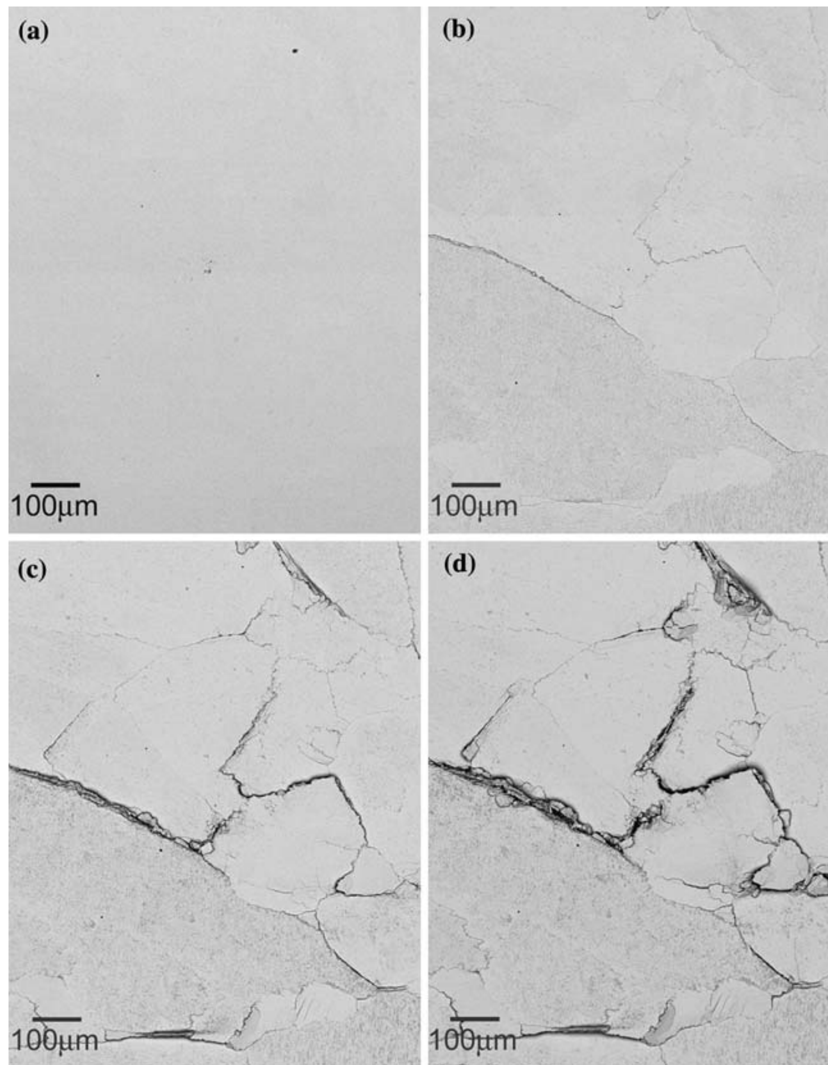

Fig. 1. Development of cracks in a Sn-3.8wt.%Ag-0.7wt.%Cu sample during thermal cycling: (a) before test, (b) after 100 cycles, (c), after 1,000 cycles, and (d) after 3,000 cycles.

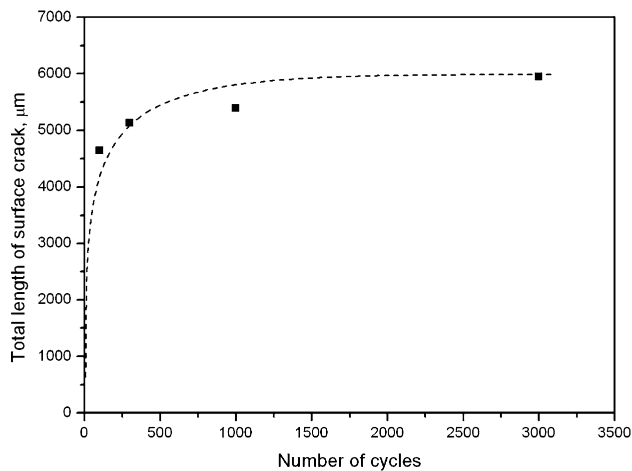

Fig. 2. Total length of surface cracks as a function of number of cycles.

total surface crack length–number of cycles relationship is presented in Fig. 2 and shows the virtual cessation of surface crack growth after some 500 cycles, when the total, overall crack length is about 5 mm.

In greater detail, the cracks had various forms (Fig. 3). In Fig. 3a, cracks a, b, c, and d are normal to cracks e, f, and g. Growth of these cracks segmented the solder and caused the originally flat polished surface to become undulated. The cracks e and f produced steps, which can also be found in Fig. 3b. The crack a in Fig. 3b produced a step raising about 40 μm. Crack opening can be more than 30 μm (a in Fig. 3c) and resulted in fragmentation of the surface of the solder (Fig. 3d). In more severe cases, as shown in Fig. 3e, fine particles ranging from several to 20 μm diameter were produced. The solder was also heavily deformed

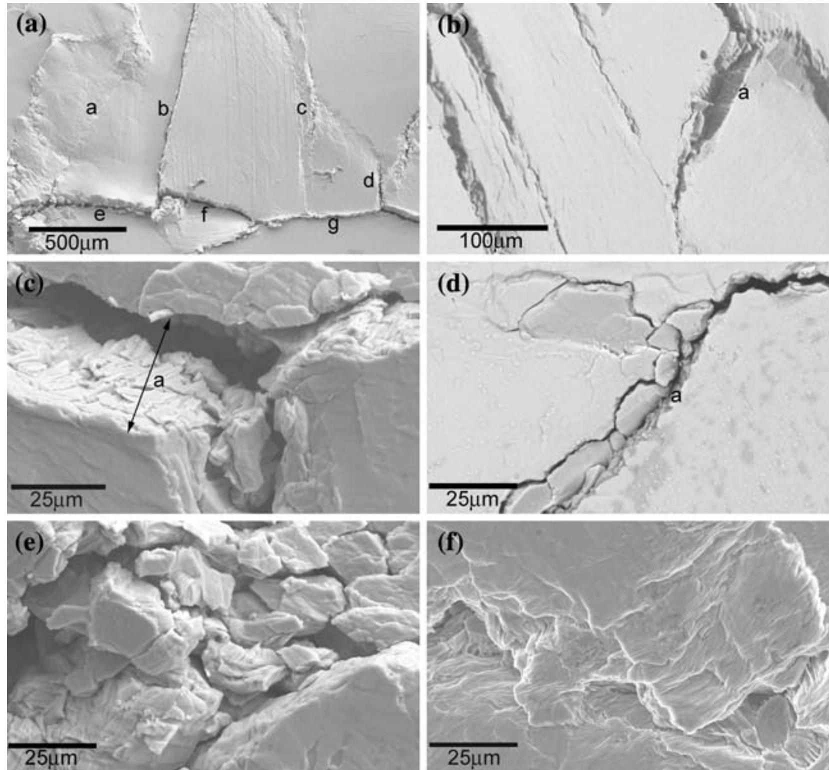

Fig. 3. Cracks in Sn-3.8wt.%Ag-0.7wt.%Cu after 300 cycles. (a) Cracks *a*, *b*, *c*, and *d* grow vertically; *e*, *f*, and *g* horizontally; and *e* and *f* produce steps. (b) Crack *a* produced a step raising about 40 μm. (c) Cracking produced an opening 30-μm wide, *a*. (d) Solder fragments beside crack *a*. (e) Fragments of solder produced by cracking. (f) Stretching lines along cracks.

during the cycling, and Fig. 3f shows a band of stretch lines along cracks.

Sectioning revealed that cracks grew into the interior of the material to up to 300 μm in depth (Fig. 4). Figure 5 shows the distribution of individual crack depths (each point represents the depth of a single crack) and average crack depth, with the number of cycles, respectively. Additional cracks are formed as cycling continues. The average depth increases from 4 μm after 100 cycles to 78 μm after 3,000 cycles, and the maximum depth increases

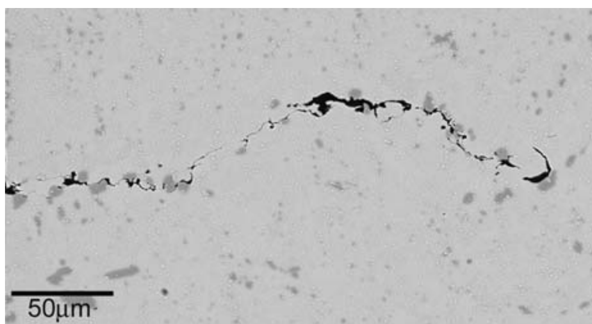

Fig. 4. Crack growth into the interior of Sn-3.8wt.%Ag-0.7wt.%Cu after 3,000 cycles in a sample sectioned and polished after thermal cycling.

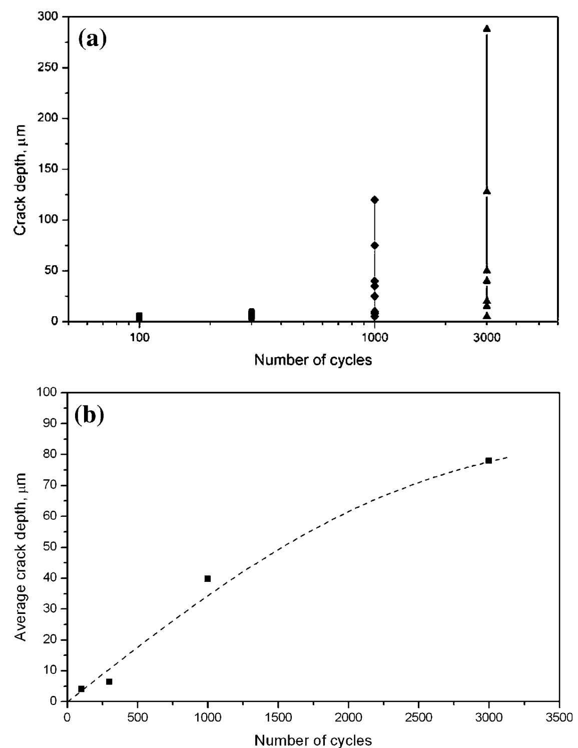

Fig. 5. (a) Range of cracking depth after 100 cycles, 300 cycles, 1,000 cycles, and 3,000 cycles. (b) Average crack depth as a function of the number of cycles.

from 6 μm after 100 cycles to 288 μm after 3,000 cycles. While the crack length on surface does not change significantly during the cycling from 100 to 3,000 cycles (Fig. 2), the maximum depth of cracks growing toward the interior increases by almost two orders during this period.

The displacement in the solder was revealed by cycling a freestanding block containing surface grinding lines, which were originally straight (Fig. 6a). After 300 cycles, line A was distorted due to grain boundary sliding parallel to the surface. Dividing this line into three sections, a-b, b-c, and c-d (Fig. 6b), the section b-c has experienced substantial deformation. The vertical separation h, of points b and c, is 7.5 μm, and the horizontal displacement, D, is 8.5 μm. Thus, a shear strain, γ ($\gamma = D/h$), of about 110% has been produced locally. After 1,000 cycles, a similar shear strain was produced and cracking resulted in a fracture, e, of grinding line B (Fig. 6c). This indicates that, without any externally applied stress or strain, thermal cycling can impose substantial cyclic strains that result in cracking.

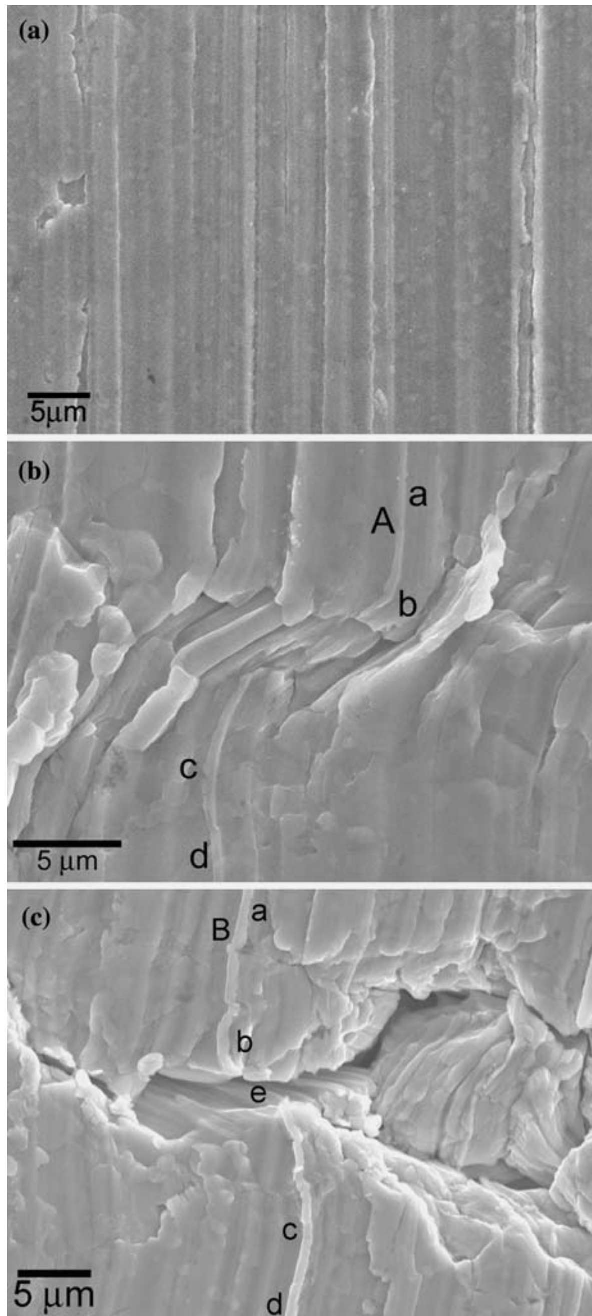

Fig. 6. Displacement caused by thermal cycling in Sn-3.8wt.%Ag-0.7wt.%Cu. (a) Grinding lines before thermal cycling. (b) Curved grinding line A after 300 cycles and a shear strain of 110% between *b* and *c*. (c) A break, *e*, of grinding line B and a shear strain of 100% between *b* and *c* after 1,000 cycles.

Figure 7 presents the shear strains developed during thermal cycling, with a temperature range of 95°C, from a grain boundary of 20 μm length when a grain with an orientation of <100> contacts with the grains in the crystalline orientations listed in Table I. The shear strain, γ, increases with the inverse of the distance to grain boundary, h ($\gamma = D/h$), where D is the displacement along the grain boundary, ranging

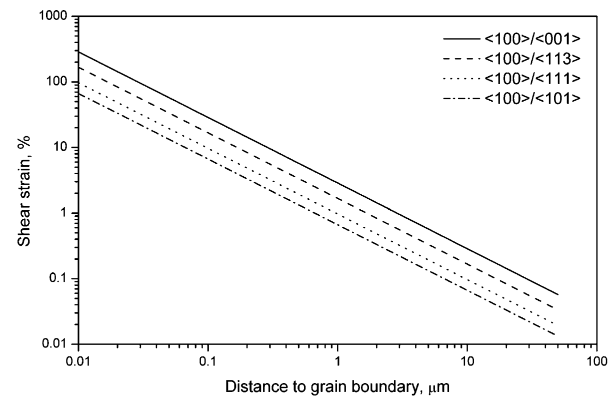

Fig. 7. Shear strains caused by thermal cycling with a temperature range of 95°C as a function of the distance to a grain boundary of 20-μm length when a grain with a crystalline orientation of <100> contacts, respectively, with the grains in the crystalline orientations listed in Table I.

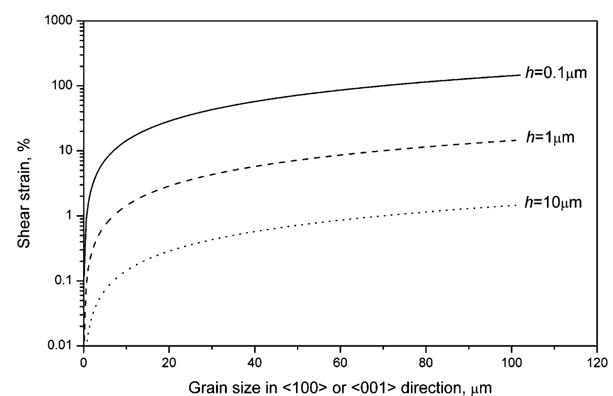

Fig. 8. Shear strain as a function of grain size at different distances, h, to the grain boundary, when two grains are in a <100>/<001> contact and cycled with a temperature range of 95°C.

from about 1% at $h = 1\ \mu$m to several tens percent at $h = 0.1\ \mu$m under the current cycling conditions. According to the orientation combination, the shear strain may vary by a factor of about 5. Shear strain, γ, is proportional to displacement, D. This implies that, when two grains are in a contact with the crystalline orientation, which has thermal expansion mismatch, the larger the grains, the greater the shear strain imposed (Fig. 8). Grain size is expressed as its dimension along the <100> or <001> direction, which is in a <100>/<001> contact with another grain. At the same distance from grain boundary, shear strain increases linearly with grain size.

Similar cracks also occurred in the blocks of pure Sn (Fig. 9a), Sn-3.5wt.%Ag (Fig. 9b), and Sn-0.5wt.%Cu (Fig. 9c), indicating the commonality of the phenomenon in Sn-based solders during thermal cycling. Figure 10a shows a sample of pure tin after 100 cycles, revealing cracks and surface undulation on the originally flat surface. Figure 10b is an electron-backscatter diffraction (EBSD) image of the same area, showing that cracks occurred along grain boundaries and that grain boundaries also outlined the regions subjected to different amounts of deformation, which resulted in surface undulation.

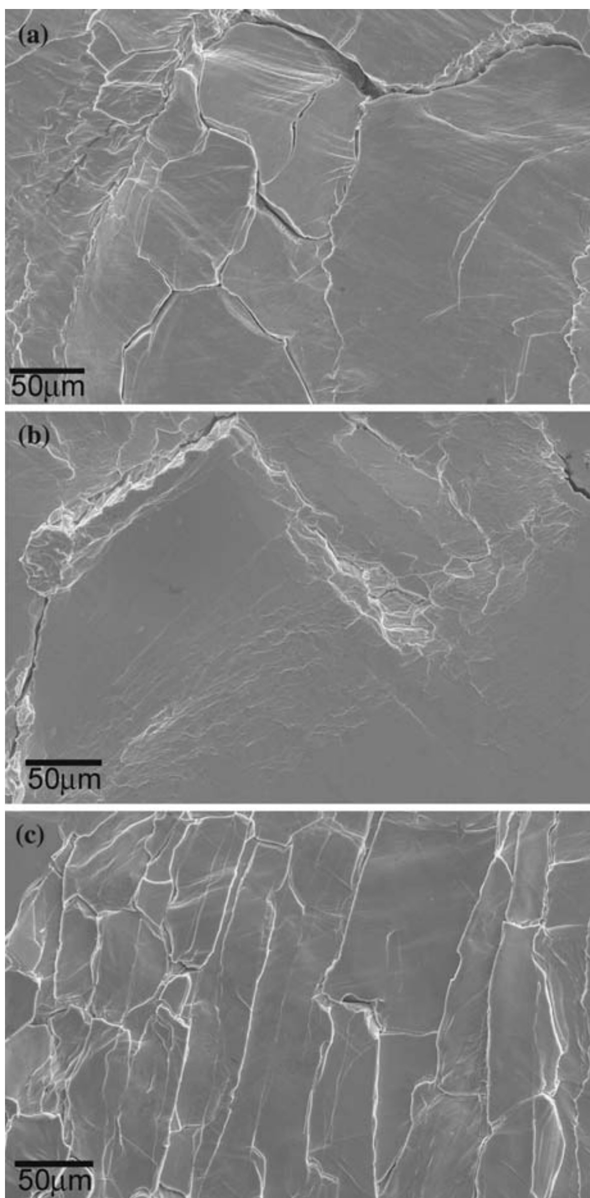

Fig. 9. Cracks after 3,000 cycles in (a) pure Sn, (b) Sn-3.5wt.%Ag, and (c) Sn-0.5wt.%Cu.

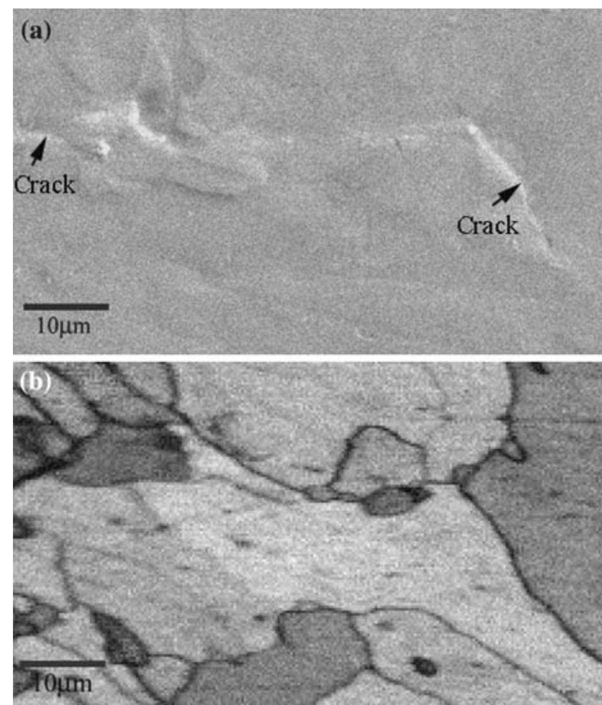

Fig. 10. (a) Cracks and surface undulation in pure tin after 100 cycles and (b) EBSD image of the same area.

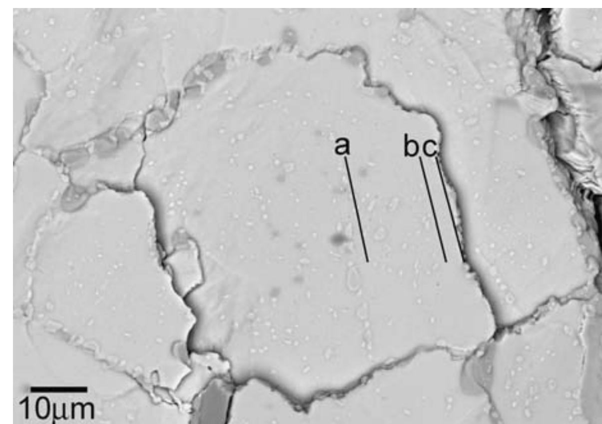

Fig. 11. Precipitation of intermetallics along cracks after 3,000 cycles in Sn-3.8wt%Ag-0.7wt%Cu. The EDS microanalysis was performed along paths a, b, and c.

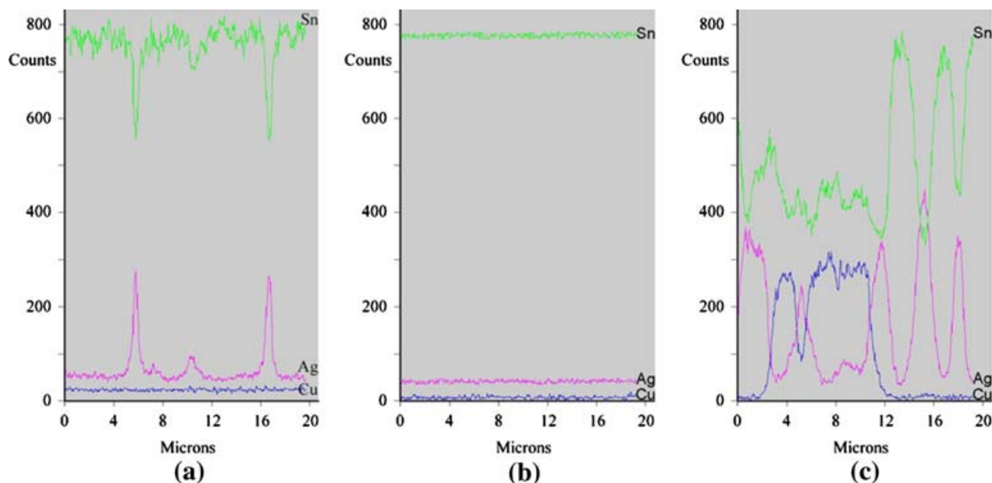

Fig. 12. EDS microanalysis along the paths a, b, and c shown in Fig. 11.

Intermetallics were precipitated in the vicinity of the cracks (Fig. 11). Energy-dispersive x-ray spectrometer (EDS) microanalysis was performed along the paths *a* (in the body of the grain), *b* (in the vicinity, ~5 μm, of the grain boundary), and *c* (adjacent to the grain boundary). The composition along the path, *a*, is the distribution of tin-silver/tin-copper intermetallics (Fig. 12a), and the number of peaks in the silver content suggests that four Sn-Ag particles are encountered on this traverse. The copper-containing intermetallics appear dark. Along the path *b*, as indicated by the Ag and Cu levels, no intermetallics are observed (Fig. 12b). However, along the path *c*, the high content of silver and copper indicates further precipitation at the grain boundary itself (Fig. 12c). Thus, during thermal cycling, an intermetallic-depleted zone is formed beside cracks, while intermetallics are precipitated along cracks themselves, as shown in Fig. 13. However, the roles of the precipitate-free zone (PFZ) and the intermetallics precipitated adjacent to the cracks are unclear.

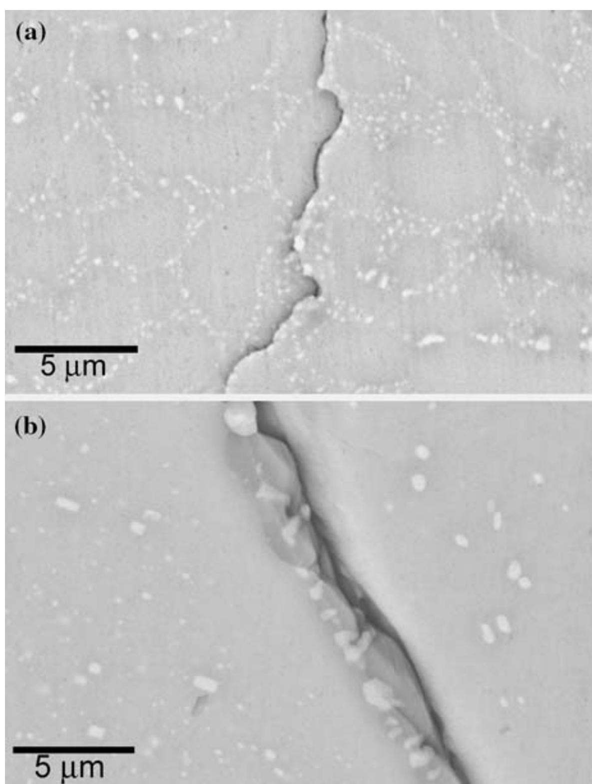

Fig. 13. Development of PFZ beside crack and precipitation of intermetallics along crack in Sn-3.8wt.%Ag-0.7wt.%Cu: (a) after 10 cycles and (b) after 300 cycles.

Effects of Initial Microstructure

Rapid cooling after casting slightly reduces crack formation, as compared with air or furnace cooling. Figure 14 shows the initial microstructures and cracking after 1,000 cycles in Sn-3.8wt.%Ag-0.7wt.%Cu prepared by (a) water quenching (80°C s^{-1}), (b) air cooling (0.2°C s^{-1}), and (c) furnace cooling (0.004°C s^{-1}). With reduced cooling rate, the Sn-Ag and Sn-Cu intermetallics coarsened. Cracks may develop along the interfaces between tin matrix and coarsened intermetallic particles, as shown by the Sn-Cu intermetallic particle *a* in Fig. 14c.

Figure 15a shows the differences in individual crack depths for water-quenched, air-cooled, and furnace-cooled samples after 1,000 cycles and indicates the slight superiority of the fastest cooled microstructure. This is confirmed in Fig. 15b, which shows that the *average* crack depth in the water-quenched sample is about a half that produced in the furnace-cooled specimen.

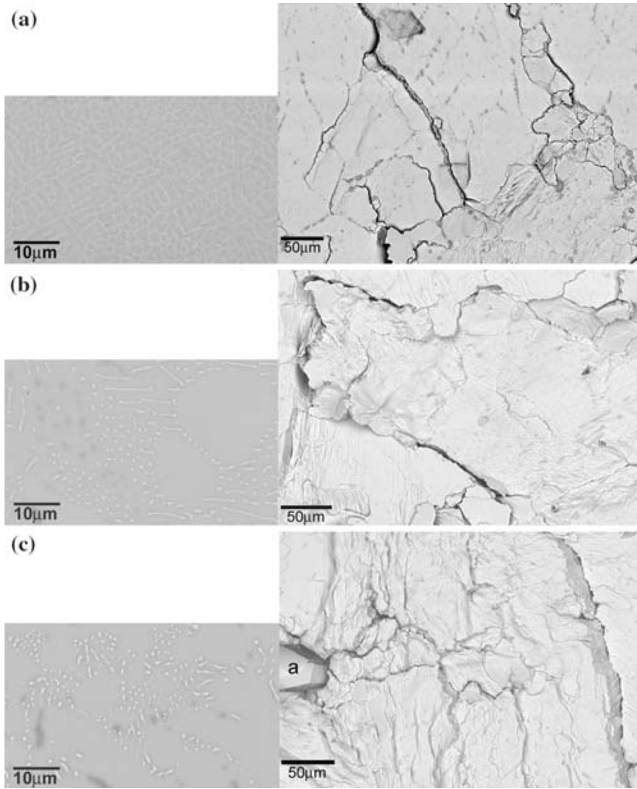

Fig. 14. Initial microstructure of, and cracks after, 1,000 cycles in Sn-3.8wt.%Ag-0.7wt.%Cu prepared by (a) water quenching, (b) air cooling, and (c) furnace cooling.

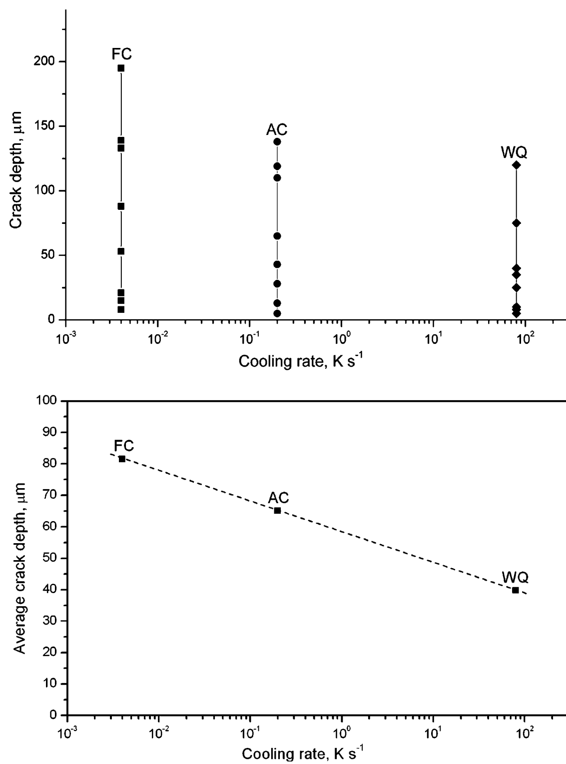

Fig. 15. (a) Range of cracking depth after 3,000 cycles for the Sn-3.8wt.%Ag-0.7wt.%Cu samples prepared by different cooling rates. (b) Effect of cooling rate on average cracking depth.

Effect of Temperature Profile

While the influence of temperature range can be directly equated with strain range, in the fatigue sense, the mean and temperature extremes may have a less obvious effect. With a constant temperature range, the amount of damage falls as the mean (or maximum) temperature of the cycle is reduced, and there is an indication that there is a thermally activated component of growth. Figure 16 shows the cracks in Sn-3.8wt.%Ag-0.7wt.%Cu formed by thermal cycling, with fixed temperature

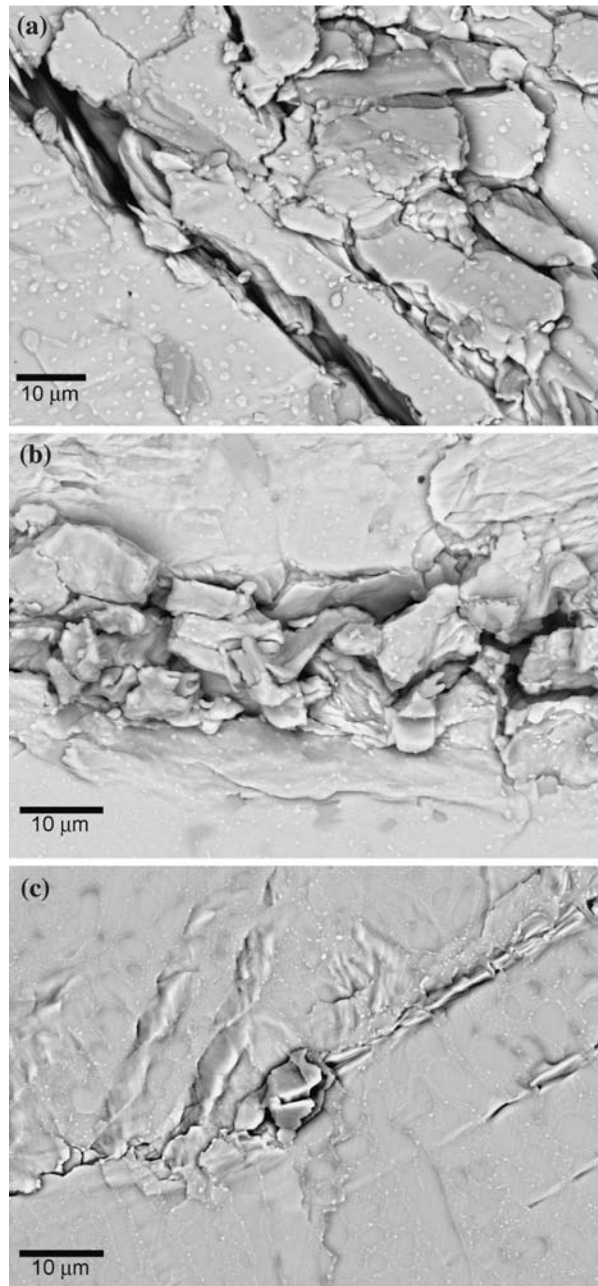

Fig. 16. Cracks in Sn-3.8wt.%Ag-0.7wt.%Cu after 1,000 cycles when cycled from (a) 30°C to 125°C, (b) from −5°C to 90°C, and (c) from −40°C to 55°C.

ranges from 30°C to 125°C, from −5°C to 90°C, and from −40°C to 55°C. Fewer surface cracks, with a smaller opening, were produced as the mean and maximum temperatures decreased.

The reduced damaged associated with lower maximum or mean temperatures can be attributed to an increase in modulus with falling temperature. For a fixed temperature (or total strain) range, the elastic component increases at the expense of the plastic component, which is the principal factor in determining damage.

Crack penetration into the interior of the sample was also markedly reduced (Fig. 17a), and plotting the cracking rate (defined as the average crack depth divided by the number of cycles) versus the reciprocal of the maximum temperature (Fig. 17b) indicates the existence of a thermally activated component of crack growth, although no attempt has been made to identify the precise mechanism involved. Time-dependent processes can occur even during continuous cycling if the strain rate is not high. An estimate of the strain rates in the present tests is $3 \times 10^{-6} - 9 \times 10^{-5}\ s^{-1}$ according to the location. These would be regarded as low and therefore susceptible to time-dependent effects.

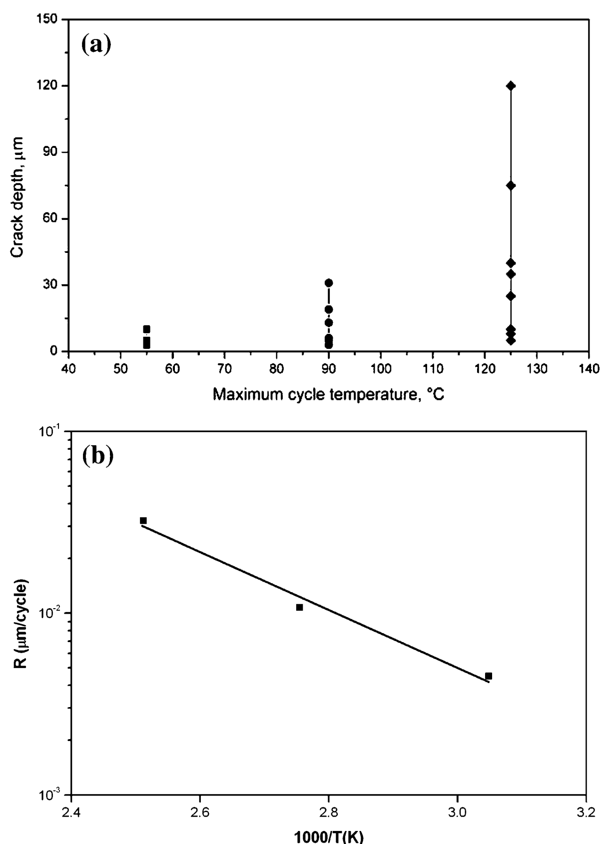

Fig. 17. (a) Range of cracking depth into interior of specimen after 1,000 cycles during thermal cycling from −40°C to 55°C, −5°C to 90°C, and 30°C to 125°C, respectively. Each point represents a single crack. (b) Cracking rate, R (μm/cycle), as a function of reciprocal temperature, $1/T$ (K).

Influence of Aging

To isolate pure isothermal from cyclic effects, aging at 125°C for 200 h, equivalent to the highest temperature of thermal cycling and a time span of 100 cycles, was performed. Comparison of Fig. 18a and b shows that aging caused some precipitation of second phases but no cracking. However, subsequent cycling from 30°C to 125°C for 100 cycles produced cracks (Fig. 18c). This demonstrates the necessity of a cyclic component of temperature to cause cracking.

It has been assumed throughout this study that the allotropic transformation to α tin at 13°C does not take place during thermal cycling because the

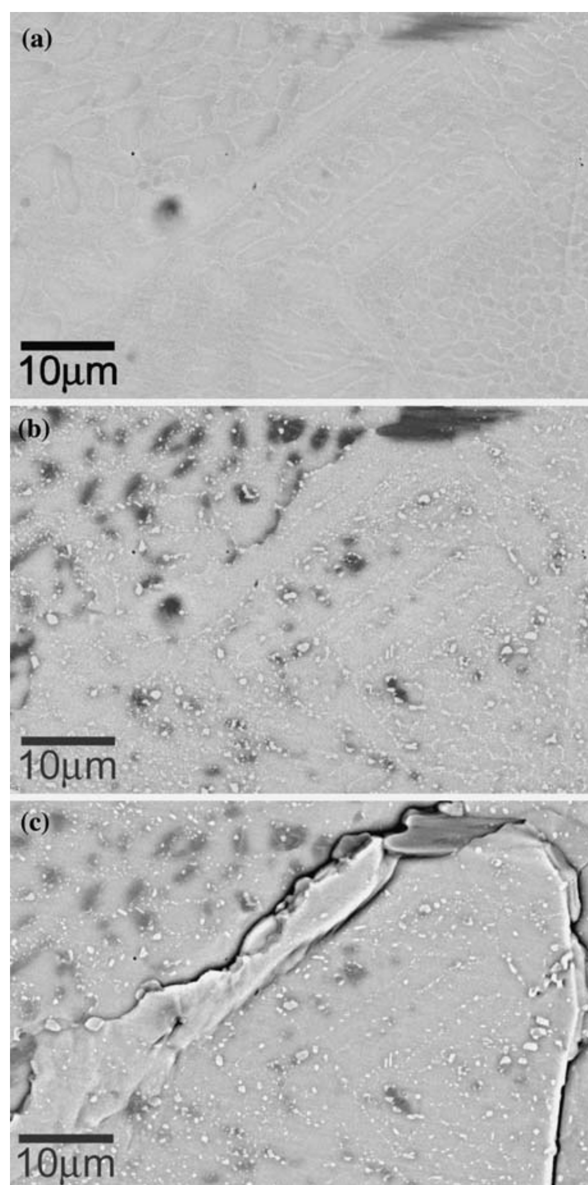

Fig. 18. (a) An as-cast Sn-3.8wt.%Ag-0.7wt.%Cu sample, (b) after aging at 125°C for 200 h and (c) then cycled from 30°C to 125°C for 100 cycles producing cracks.

necessary incubation period is not attained.[20] For pure tin and tin-0.5wt.%Cu, this period is at least several months, and for the silver-containing alloys, it is considerably longer and there is some debate as to whether it occurs at all.

CONCLUSIONS

Tin-based, lead-free solders, such as Sn-Ag-Cu, may experience significant damage when exposed to fluctuating temperature. The anisotropy of tin in thermal expansion and modulus causes shear strains along grain boundaries when there is a temperature variation. These strains increase exponentially as a function of the proximity to the grain boundary and increase linearly with grain size. Repeated cycling causes crack initiation on the surface and subsequent penetration into the interior of the sample. The maximum depth of cracks increases linearly with the number of cycles and is reduced by higher cooling rates and a lower temperature peak of the thermal cycle. Precipitate-free zones are produced in the vicinity of cracks, although their role in the overall process is unclear. A cyclic element of temperature is essential; prolonged isothermal exposure results only in microstructural coarsening, with no cracking.

REFERENCES

1. P.M. Hall, T.D. Dudderar, and J.F. Argyle, *IEEE Trans. Compon. Hybrids Manuf. Technol.* 6, 544 (1983).
2. X.W. Liu and W.J. Plumbridge, *Mater. Sci. Eng. A* 362, 309 (2003).
3. H.D. Solomon, *IEEE CHMT* 9, 423 (1986).
4. N.F. Enke, T.J. Kilinski, S.A. Schroeder, and J.R. Lesniak, *IEEE CHMT* 12, 459 (1989).
5. S. Vaynman, and M.E. Fine, in *Solder Joint Reliability*, ed. J.H. Lau (New York: Van Nostrand Reinhold, 1991), pp. 334–360.
6. H. Jiang, R. Hermann, and W.J. Plumbridge, *J. Mater. Sci.* 31, 6455 (1996).
7. J. Chin, H. Mavoori, M.E. Fine, B. Moran, and L.M. Keer, *NEPCON WEST 97 Conf.* (Anaheim, CA: Reed Exhibition Companies, 1997), pp 15–23.
8. H. Conrad, Z. Guo, Y. Fahmy, and D. Yang, *J. Electron. Mater.* 28, 1062 (1999).
9. P.M. Hall, *IEEE Trans. Comp. Hybrids Manuf. Technol.* 7, 314 (1984).
10. Q. Guo, E.C. Cutiongco, L.M. Keer, and M.E. Fine, *J. Electron. Packag.* 114, 145 (1992).
11. P. Hacke, A.F. Sprecher, and H. Conrad, *J. Electron. Packag.* 115, 153 (1993).
12. R.G. Ross Jr., *J. Electron. Packag.* 116, 69 (1994).
13. Y.H. Pao, S. Badgley, R. Govila, and E. Jih, *Fatigue of Electronic Materials, ASTM STP 1153*, ed. S.A. Schroeder (Philadelphia, 1994), pp. 60–81.
14. C.H. Raeder, R.W. Messler, and L.F. Coffin Jr., *J. Electron. Mater.* 28, 1045 (1999).
15. J.G. Lee, A. Telang, K.N. Subramanian, and T.R. Bieler, *J. Electron. Mater.* 31, 1152 (2002).
16. F. Guo, J.G. Lee, T.P. Hogan, and K.N. Subramanian, *J. Mater. Res.* 20, 364 (2005).
17. K.N. Subramanian and J.G. Lee, *J. Mater. Sci.: Mater. Electron.* 15, 235 (2004).
18. W.J. Plumbridge and Y. Kariya, *Fatigue Fract. Eng. Mater. Struct.* 27, 723 (2004).
19. *Metals Handbook*, 2nd ed., ed. J.R. Davis (Materials Park, OH: ASM International, 1998), p. 94.
20. Y. Kariya, N. Williams, C.R. Gagg, and W.J. Plumbridge, *J. Mater.* 53, 39 (2001).